

# Distribution of Ca<sup>2+</sup>-Activated K<sup>+</sup> Channel Isoforms along the Tonotopic Gradient of the Chicken's Cochlea

Kevin P. Rosenblatt,<sup>†</sup> Zhong-Ping Sun,\* Stefan Heller,\* and A. J. Hudspeth\*

\*Howard Hughes Medical Institute and Laboratory of Sensory Neuroscience The Rockefeller University New York, New York 10021-6399

## Summary

In some cochleae, the number and kinetic properties of Ca<sup>2+</sup>-activated K<sup>+</sup> (K<sub>Ca</sub>) channels partly determine the characteristic frequency of each hair cell and thus help establish a tonotopic map. In the chicken's basilar papilla, we found numerous isoforms of K<sub>Ca</sub> channels generated by alternative mRNA splicing at seven sites in a single gene, *cSlo*. In situ polymerase chain reactions demonstrated *cSlo* expression in hair cells and revealed differential distributions of K<sub>Ca</sub> channel isoforms along the basilar papilla. Analysis of single hair cells by the reverse transcription polymerase chain reaction confirmed the differential expression of channel variants. Heterologously expressed *cSlo* variants differed in their sensitivities to Ca<sup>2+</sup> and voltage, suggesting that the distinct spatial distributions of *cSlo* variants help determine the tonotopic map.

## Introduction

The cochlea is tonotopically mapped: the hair cells at each position along the organ are most sensitive to a particular frequency (reviewed in Roberts et al., 1988; Hudspeth, 1989). This usually monotonic tuning gradient is established in different species by a variety of means, including the mechanical properties of auditory accessory structures such as the basilar and tectorial membranes (reviewed in von Békésy, 1960) as well as those of the hair cells themselves (Frishkopf and DeRosier, 1983; Holton and Hudspeth, 1983; Freeman and Weiss, 1990). In the ears of many amphibians (Ashmore, 1983; Lewis and Hudspeth, 1983a, 1983b), reptiles (Crawford and Fettiplace, 1980, 1981; Fuchs and Evans, 1988), and birds (Fuchs et al., 1986), each hair cell is additionally frequency tuned by an intrinsic electrical resonance mechanism. Upon stimulation, such a cell exhibits exponentially damped oscillations in its membrane potential, the frequency of which lies near the cell's characteristic, or best response, frequency.

Electrical frequency tuning depends on ionic currents across the basolateral membrane. In conjunction with a cell's membrane capacitance, the currents through two types of channels, L-type Ca<sup>2+</sup> channels and large conductance K<sub>Ca</sub> channels, are necessary and sufficient for electrical resonance (Lewis and Hudspeth, 1983a, 1983b; Art and Fettiplace, 1987; Hudspeth and Lewis, 1988a, 1988b). Resonance may be explained by a model

in which several successive events occur during each cycle of oscillation (Hudspeth and Lewis, 1988b; Wu et al., 1995). Depolarization first opens the voltage-dependent Ca<sup>2+</sup> channels, augmenting the inward current. The local cytoplasmic accumulation of Ca<sup>2+</sup> activates K<sub>Ca</sub> channels, which open after a brief delay. These K<sup>+</sup> channels pass a large outward current, resulting in rapid membrane repolarization, Ca<sup>2+</sup> channel closure, decreased Ca<sup>2+</sup> influx, falling Ca<sup>2+</sup> concentration, and finally K<sub>Ca</sub> channel closure. Electrical resonance acts as an electrical filter (Crawford and Fettiplace, 1980), maximizing a hair cell's response to sounds of frequencies near the resonant frequency and attenuating its response at other frequencies. Electrical resonance thus confers sharp frequency selectivity upon hair cells (Crawford and Fettiplace, 1981).

The model of electrical resonance indicates that the electrical resonant frequency is determined by the numbers of channels and the kinetic properties of the K<sub>Ca</sub> current (Hudspeth and Lewis, 1988b). Studies performed on isolated hair cells from amphibian, reptilian, and avian inner ears have supported this suggestion (Roberts et al., 1986; Art and Fettiplace, 1987; Fuchs et al., 1990). Recordings in the turtle's cochlea have additionally indicated that the single-channel properties of the K<sub>Ca</sub> channels vary from cell to cell (Art et al., 1995; Wu et al., 1995). The molecular basis of the variation in K<sub>Ca</sub> channel kinetics, however, is not understood.

Investigations in other experimental systems provide insight into the molecular mechanism by which the kinetic properties of K<sub>Ca</sub> channels might be adjusted. These channels are the products of *Slowpoke* genes, which have been cloned from tissues of *Drosophila melanogaster* (*dSlo*; Atkinson et al., 1991), mouse (*mSlo*; Butler et al., 1993), and human (*hSlo*; Dworetzky et al., 1994; Pallanck and Ganetzky, 1994; Tseng-Crank et al., 1994). Slo channels belong to the subfamily of maxi-K channels (reviewed in Latorre et al., 1989), which are large conductance K<sup>+</sup> channels activated by intracellular Ca<sup>2+</sup> and depolarization; the K<sub>Ca</sub> channels characterized in vertebrate hair cells evidently fall into the same classification (Lewis and Hudspeth, 1983a; Art and Fettiplace, 1987; Hudspeth and Lewis, 1988b; Fuchs et al., 1990; reviewed in Fuchs, 1992). Slo channels exhibit extensive sequence variability produced by alternative splicing of their mRNAs (Atkinson et al., 1991; Adelman et al., 1992; Butler et al., 1993; Tseng-Crank et al., 1994). Many of these splice variants give rise to channels that differ in physiological properties such as single-channel conductance, kinetics, and Ca<sup>2+</sup> sensitivity (Adelman et al., 1992; Lagrutta et al., 1994; Tseng-Crank et al., 1994). We therefore sought to determine whether the functional diversity in K<sub>Ca</sub> channels in hair cells of the chicken's inner ear is generated through alternative splicing of their mRNAs.

## Results

To investigate the molecular basis of electrical frequency tuning, we cloned and analyzed cDNAs encoding numerous splice variants of K<sub>Ca</sub> channels from the

<sup>†</sup> Present address: Medical Scientist Training Program, University of Texas Southwestern Medical Center, 5323 Harry Hines Boulevard, Dallas, Texas 75235.

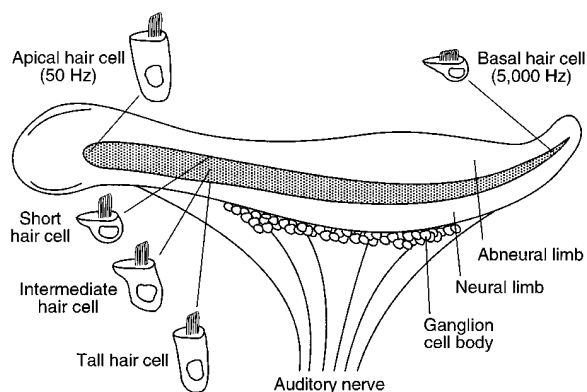


Figure 1. Tonotopic and Morphological Gradients of the Chicken's Cochlea

Schematic illustration of the chicken's cochlea. In an adult chicken, the cochlea is a 5 mm long tubular structure comprising the basilar papilla (stippled), the tegmentum vasculosum (a vascularized secretory tissue), three scalae (fluid-filled compartments), and the cochlear ganglion (Hirokawa, 1978; Tanaka and Smith, 1978). The avian homolog of the mammalian organ of Corti, the basilar papilla is an auditory epithelium containing about 10,000 hair cells and twice as many supporting cells (Tilney et al., 1986) but no neuronal cell bodies. It rests atop a mechanically tuned basilar membrane (von Békésy, 1960; Gummer et al., 1987) that forms the base of the scala media. The hair cells are arranged in a tonotopic gradient along the cochlea, responding to sounds whose frequencies range from 50–5000 Hz (Gray and Rubel, 1985; Manley, 1996); low frequencies are detected at the organ's apical end and high frequencies at its base. These hair cells also manifest two morphological gradients. First, hair cells at the apical end of the cochlea have relatively few, long stereocilia and those at the base almost 10-fold as many shorter stereocilia (reviewed in Tilney et al., 1992). Second, there is a gradation in the size and shape of hair-cell somata across the width of the basilar papilla, from tall hair cells overlying the cochlear ganglion to short cells on the abneural edge (Tanaka and Smith, 1978). The tall and short hair cells are dominantly innervated by afferent and efferent nerve fibers, respectively (Hirokawa, 1978; Tanaka and Smith, 1978); they are believed to be analogous to the inner and outer hair cells, respectively, of the mammalian cochlea (Manley et al., 1989).

basilar papilla, or sensory epithelium, of the chicken's cochlea (Figure 1). We elected to use this preparation for three reasons. First, the electrophysiological properties of  $K_{Ca}$  channels (Fuchs and Evans, 1990; Murrow, 1994) and their contribution to electrical tuning (Fuchs et al., 1986) have been thoroughly characterized in this organ. Second, because the chicken's cochlea has a well-defined tonotopic map (Chen et al., 1994; Jones and Jones, 1995; reviewed in Manley, 1996), the properties of  $K_{Ca}$  channels in this organ can readily be related to the electrical tuning of the hair cells in which these channels are expressed. Finally, because it is used extensively for studies of aural morphogenesis (reviewed in Tilney et al., 1992) and tonotopic map development (reviewed in Manley et al., 1987), the chicken's cochlea is an excellent preparation in which to investigate the development of electrical resonance at the molecular level.

#### Molecular Structure of *cSlo* cDNAs Derived from the Brain and Basilar Papilla

To isolate cDNAs encoding the chicken's large conductance  $K_{Ca}$  channels, we took advantage of the greater

than 50% identity among the members of the *Slo* family to design three sets of degenerate PCR primers. Because  $K_{Ca}$  channels are expressed in the brains of many species (reviewed in Latorre et al., 1989; Hinrichsen, 1993), we chose the brain as our initial source of mRNA. Using the degenerate primers in the RT-PCR (reverse transcription polymerase chain reaction), we produced three overlapping PCR products constituting 2.9 kbp of coding sequence that was highly similar to that of the mouse or human. These amplification products were then used as probes to screen a chicken brain cDNA library. Extensive oversampling of the library yielded eight cDNA clones that contained *Slo* sequence. The overlapping PCR and library cDNA clones indicated the existence of at least ten transcripts, 4.0–4.6 kbp in length, that encode proteins ranging in length from 1105 to 1231 amino acids. Northern blot analysis demonstrated that the predominant transcripts in the eye, brain, and cochlea were 4–4.5 kbp in length (data not shown), indicating that the overlapping cDNAs are likely to represent full-length transcripts. A full-length cDNA (cB1) encoding a protein 1146 amino acids in length was constructed from three overlapping cDNA clones (Figure 2); similar results have recently been obtained by two other groups (Jiang et al., 1997; accompanying paper, Navaratnam et al., 1997 [this issue of *Neuron*]).

Based on hydropathy and sequence analyses of the coding sequence (data not shown), the c*Slo* protein contains eleven hydrophobic segments (S0–S10) with high potential for  $\alpha$ -helical structure (Figures 2 and 3A). Seven of these segments (S0–S6) are located in the amino-terminal third of the sequence. The remaining four segments (S7–S10) occur in the carboxyl terminus and match equivalent domains of the mammalian channels (Butler et al., 1993; Tseng-Crank et al., 1994).

The predicted c*Slo* product exhibits extensive sequence similarity to the other *Slo* channels. Excluding alternative exons, c*Slo* is 95% identical to m*Slo* and h*Slo*, differing in only 44 amino acid residues. Most of these differences occur in the amino-terminal region, upstream of the S1 domain, and in the carboxy-terminal region, between the S7 and S10 domains (Figure 2). c*Slo* displays only 55% identity to d*Slo*, with most of the differences located in the extreme amino- and carboxy-terminal domains and between the S8 and S9 domains.

As for the other *Slo* channels, four methionine codons occur near the 5' end of the coding sequence (Figure 2). Because each of the first three codons occurs within a consensus sequence for eukaryote ribosomal binding (Kozak, 1991), several of them may serve as initiation sites for translation. However, as for the human channel (Tseng-Crank et al., 1994), the third methionine codon offers the best consensus and may thus be the preferred initiation site.

To determine whether the *cSlo* gene encodes the  $K_{Ca}$  channels expressed in the chicken's basilar papilla, we initially used total RNA isolated from this tissue and specific PCR primers to verify that *cSlo* occurs in the cochlea. Using the 5' *cSlo* probe originally isolated from the brain by the degenerate PCR, we then screened a cDNA library constructed from the embryonic basilar papilla. Two clones were identified. Clone cSE2 extends from the S1 domain to the poly(A) tail; clone cSE5 extends from between the S2 and S3 domains to the poly(A)



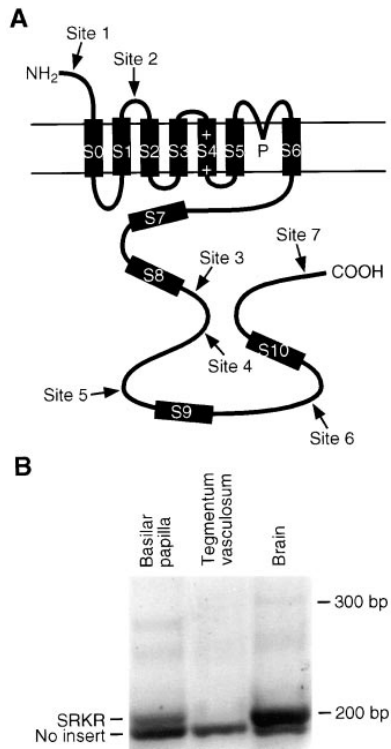


Figure 3. Alternative Splicing of *cSlo* mRNA

(A) Proposed membrane topology of *cSlo* indicating the regions of protein diversity generated by alternative mRNA splicing. The transmembrane  $\alpha$  helices, S0–S6, and the four carboxy-terminal hydrophobic domains, S7–S10, are represented by black rectangles. The two parallel lines represent the lipid bilayer; the extracellular surface is uppermost. The locations of the hydrophobic segments are based on the model of Wallner et al. (1996). The arrows refer to the regions of protein diversity and are named for the corresponding RNA splice sites. Note that two of these, sites 1 and 2, give rise to regions of protein diversity that are predicted to occur on the external membrane surface.

(B) RT-PCR analysis of splice site 3. Total RNA samples from the chicken's brain, basilar papilla, and tegmentum vasculosum were used for splice site-specific RT-PCR analysis. The Southern blot shows the PCR fragments generated with a primer pair that flanks the splice sites and thus amplifies the full complement of alternative exons. To ensure the specificity of the PCR products, the blot was probed with an internal oligonucleotide that recognizes all splice variants generated at this site. The data demonstrate that *cSlo* is expressed in the three tissues and that extensive alternative splicing of this gene occurs in the brain and basilar papilla. The arrows point to the two predominant products expressed at site 3 in the various tissues, which correspond to the SRKR and insertless variants. The blots additionally indicate that the relative abundances of the different mRNA species differ between tissues.

tail. In their overlapping region, these clones differ by only a 12 bp insert in the latter (site 3 in Table 1).

#### Detection of *cSlo* mRNA by In Situ Hybridization and In Situ PCR

In an effort to demonstrate the expression of *cSlo* mRNA in hair cells, we used conventional riboprobes 0.8–2 kbp in length to perform in situ hybridizations on late embryonic (E16–E18) basilar papillae. Although the chicken's hair cells possess  $K_{Ca}$  channels at this stage

(Yang and Fuchs, 1997, Assoc. Res. Otolaryngol., abstract), we observed only weak labeling of hair cells (data not shown). To confirm the efficacy of our procedure, we conducted control experiments and demonstrated labeling of neurons in the retina (Figure 4A) and brain, as well as of skeletal and smooth muscle cells. All of these tissues have previously been shown to express *Slo* in other species (reviewed in Hinrichsen, 1993).

To achieve greater sensitivity in the detection of the *cSlo* message in hair cells, we turned to the in situ RT-PCR procedure (Nuovo, 1996), a technique that combines the exquisite sensitivity of the PCR with the cellular resolution of in situ hybridization. Using digoxigenin-labeled PCR primers to conserved regions of the *cSlo* sequence, we detected *cSlo* mRNA in hair cells as well as in the cochlear ganglion and tegmentum vasculosum (Figure 4C). No signal was obtained from supporting cells. Whereas the conventional in situ technique required 1–2 days of development to detect *cSlo* mRNA in hair cells, 10–15 cycles of PCR amplification sufficed to produce intense labeling after only 5–30 min of development. Control experiments demonstrated that the signal was primer- (Figures 4D and 5D) and mRNA-dependent (Figure 4E). As a control for cell type-specific expression, we found that PCR primers to calbindin, a  $Ca^{2+}$ -binding protein expressed in the basilar papilla (Wilson et al., 1985; Oberholtzer et al., 1988), led to labeling of hair cells and supporting cells but of neither the tegmentum vasculosum nor the cochlear ganglion (Figure 5E). Nonsense primers, forward or reverse primers alone, or primers to genes not expressed in the cochlea gave no signals (data not shown).

The same technique and *cSlo* primer pair yielded labeling patterns in the retina (Figure 4B), brain, and muscle identical to those obtained with the conventional in situ technique, demonstrating the specificity of the in situ RT-PCR technique. As in the cochlea, the conventional in situ hybridization method provided weak signals in brain and muscle only after several days of development, while the in situ RT-PCR approach yielded robust labeling in 30 min to a few hours.

#### Multiple $K_{Ca}$ Channel Isoforms Generated by Alternative mRNA Splicing

The PCR amplification products and library clones derived both from the brain and from the basilar papilla displayed greater than 90% nucleotide identity; their differences stemmed from small insertions and deletions at specific sites within the coding sequence. Because the inserts did not contain consensus splice-donor or splice-acceptor dinucleotides (Senapathy et al., 1990), we considered them true exons. The nucleotide sequence identity in the conserved regions suggested that all of the isoforms were generated by alternative splicing of a single *cSlo* gene.

The observation of extensive sequence variation at specific sites in *cSlo* cDNAs prompted us to undertake a systematic examination of the extent of alternative splicing. Because some of the splice sites found in our cDNA clones are also observed in *dSlo*, *mSlo*, and *hSlo* (Table 1), we anticipated the conservation of additional splice sites between the various species. To test for the

Table 1. Splice Variants of *cSlo*

Splice Site	Variant (Residues)	Sequence	Observed in:		
			<i>dSlo</i>	<i>mSlo</i>	<i>hSlo</i>
1	14	MKPFVSLPPPPS			
	17 <sup>a</sup>	MSNNINANLNTDSSSS		+	+
2	—	(Insertless)	+	+	+
	8	<u>S</u> RTADSLI			
3	— <sup>b</sup>	(Insertless)	+	+	+
	4	<u>S</u> RKR		+	+
	20	<u>S</u> RKRYALFVTFPSNLNPTST			+
4	—	(Insertless)	+	+	+
	3	IYF	<sup>c</sup>	+	+
	59 <sup>a</sup>	PKM <u>S</u> IYKRMKLACCFDCGR <u>S</u> ERDCSCMSGSVHSNMMDTLER AFPLSSSVNDCSTSLRAF			
5	—	(Insertless)	+	+	+
	8 <sup>a</sup>	RF <u>S</u> CPFLP			+
6	—	(Insertless)	+	+	+
	28	AKPGKLLPLVSIQEK <u>N</u> SGTHILMITEL		+	+
7	8	KYVQEDRL			+
	60 <sup>a</sup>	NSTRMNRMGQEKKWFTDEPD		+	
		NAYPRNIQIKPMSTHMANQI NQYKSTSSLIPPIREVEDEC			

Potential serine phosphorylation sites are underlined.

<sup>a</sup> These variants were observed only by RT-PCR, not among library clones.

<sup>b</sup> Because the splice site lies within a codon, the arginine residue preceding the inserts at site 3 (Figure 2) becomes a serine residue in the insertless variant.

<sup>c</sup> Although this splice site exists in *Drosophila*, no previously reported variant was encountered in our study.

presence of such sites and to isolate more alternative exons, we designed specific PCR primers to portions of *cSlo* homologous to regions that flank splice sites in the *Drosophila* (Atkinson et al., 1991), mouse (Butler et al., 1993), and human clones (Tseng-Crank et al., 1994). Using this RT-PCR strategy, we were able to detect an additional site (site 5) and to isolate numerous alternatively spliced exons expressed at the different sites in the chicken's brain and basilar papilla (Table 1).

By comparing the sequences of mouse and human *Slo* genes (Butler et al., 1993; Dworetzky et al., 1994; Pallanck and Ganetzky, 1994; Tseng-Crank et al., 1994; McCobb et al., 1995), we established that sequence diversity occurs at both the amino-terminal and carboxy-terminal domains of *Slo* genes. Several *cSlo* clones with variant 5' ends were isolated from the chicken brain library. Because these clones encode proteins beginning at three different methionine residues, sequence diversity occurs at the amino terminus of *cSlo* channels as well (Figure 2). To determine whether additional diversity exists at the *cSlo* amino terminus and to test for diversity at the carboxyl terminus, we examined the 5' and 3' ends of cDNA clones from the basilar papilla library. Using the technique of rapid amplification of cDNA ends (RACE; Frohman, 1993), we conducted PCRs with *cSlo*-specific and vector primers designed to flank the extreme 5' and 3' coding sequences of *cSlo* library clones. We found two alternative exons each at the 5' and 3' ends, indicating that alternative splicing generates diverse amino and carboxyl termini (Figure 3A and Table 1). In conjunction with the alternative exons, the diversity arising from different translation-initiation sites could produce at least four alternative amino termini.

To verify the expression of alternative exons at splice site 3, which we further characterize below, we probed Southern blots of the PCR products with internal oligonucleotides capable of recognizing all variants. The Southern analysis (Figure 3B) revealed several variants expressed at this site in the brain and basilar papilla and indicated the relative abundances of the mRNAs giving rise to each variant. The two prominent bands expressed in the brain and basilar papilla represent the 4 amino acid and insertless variants (Table 1). The insertless form of *cSlo* predominated in the tegmentum vasculosum; the SRKR variant was only marginally detectable.

Our RT-PCR analysis disclosed eleven alternative exons at seven splice sites distributed over the entire length of the message (Figure 3A and Table 1). These sites occur at the amino and carboxyl termini (sites 1 and 7, respectively), in the core of the channel (site 2), and in the putatively cytoplasmic region between domains S8 and S10 (sites 3–6). If no restrictions apply to the combination of alternative exons, 576 different K<sup>+</sup> channels could be expressed from the *cSlo* gene. Because our PCR Southern blots indicated that we isolated only a subset of the alternative exons expressed at each site, however, the total number of exons and possible exon combinations could be far greater.

#### Differential Expression of *cSlo* Isoforms in the Cochlea Revealed by In Situ RT-PCR

The presence in *hSlo* channels of a basic, 4 amino acid insert, SRKR, at a position corresponding to the *cSlo* site 3 diminishes the channels' Ca<sup>2+</sup> sensitivity (Tseng-Crank et al., 1994). Because we wished to map channel

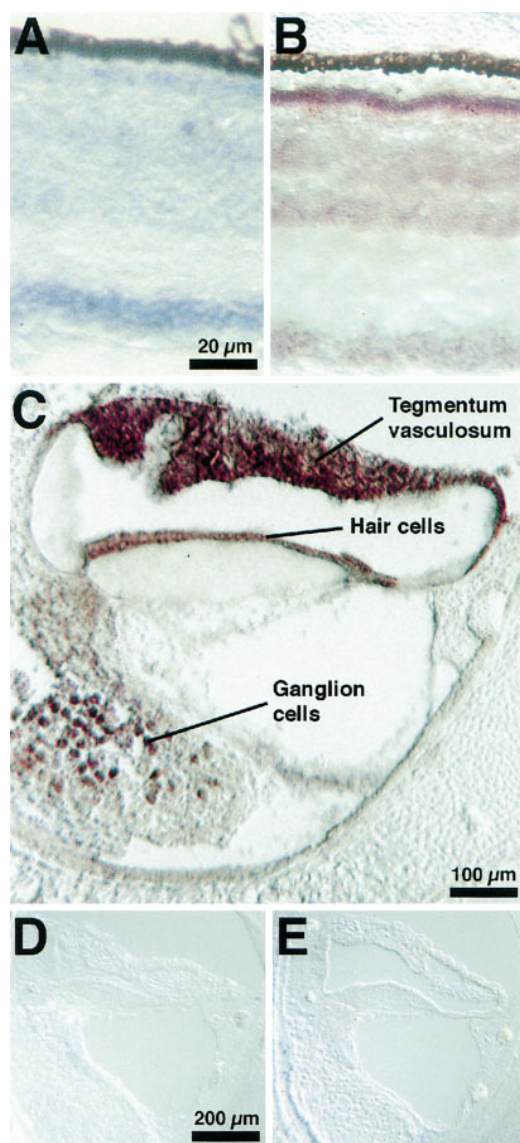


Figure 4. Expression of *cSlo* in the Chicken's Retina and Cochlea (A) Localization of *cSlo* to the retina by in situ hybridization. Digoxigenin-labeled antisense RNA derived from an 825 bp fragment encoding part of the carboxy-terminal domain was hybridized to a cryosection of the embryonic retina. The probe was detected with alkaline phosphatase-conjugated anti-digoxigenin antibodies in a color reaction. Labeling can be seen in the outer and inner nuclear layers and in the retinal ganglion layer. The section was developed for 48 hr. (B) Localization of *cSlo* to the retina by in situ RT-PCR. Digoxigenin-labeled primers were used with the direct in situ RT-PCR to detect *cSlo* mRNA in the retina. The labeling pattern is identical to that seen with the conventional hybridization technique. The section was developed for 30 min. (C) Localization of *cSlo* in the cochlea by in situ RT-PCR. The primer pair utilized in (B) was employed to localize the *cSlo* message to hair cells, ganglion cells, and the tegmentum vasculosum of the embryonic cochlea. The section was developed for 30 min. (D) Primer dependency of in situ RT-PCR localization of *cSlo* in the cochlea. In situ RT-PCR was performed on an embryonic cochlea without the labeled *cSlo* primers. No labeling was detected after 24 hr of development. (E) mRNA dependency of in situ RT-PCR localization of *cSlo* in the cochlea. The section was heated to 92°C for 5 min to inactivate the reverse transcriptase before amplification. No significant labeling was detected after 24 hr of development.

variants that were likely to have functional consequences for electrical frequency tuning, and because this 4 amino acid insert and the absence of an insert were the predominant variants found at site 3 of the chicken's basilar papilla (Figure 3B), we used the in situ RT-PCR technique to map the expression of these site 3 variants along the cochlea. Amplified cDNAs were detected either directly, by incorporation of labeled nucleotides in PCR products, or indirectly, by hybridization with labeled internal probes.

When primers that amplify the SRKR variant were used on serially sectioned embryonic cochleae, reaction product was detected only in hair cells. More importantly, the labeling was confined to hair cells in the middle third of the cochlea's length (Figure 5).

Because the chicken's tonotopic map is not fully developed at hatching (reviewed in Manley, 1996), we mapped the 4 amino acid and insertless variants at site 3 in the more mature cochleae of 1- to 2-week-old chicks. To analyze the SRKR variant, we employed the site 3-flanking primers to amplify all *cSlo* variants at this site and utilized a labeled, variant-specific probe for detection. Hair cells were strongly labeled in the apical region of the cochlea (Figure 6C), whereas much weaker labeling was observed in the ganglion cell bodies, and only marginal labeling was detected in the tegmentum vasculosum. In basal cochlear sections, the hair cells showed little or no labeling (Figure 6D); the signals in the tegmentum vasculosum and ganglion were comparable to those in the apex.

When amplifying the insertless variant, we found significant labeling in hair cells, ganglion cells, and the tegmentum vasculosum. This variant was expressed in these three cell types from the apical to the basal end of the cochlea (Figures 6A and 6B, respectively). The expression level in hair cells at the more apical regions was slightly less than that in the tegmentum vasculosum and cochlear ganglion; in more basal regions, the expression levels were more nearly equal in the three tissues.

#### Expression of Multiple $K_{Ca}$ Variants by Individual Hair Cells

As an independent confirmation of *cSlo* expression in hair cells and to determine whether more than one splice variant can be expressed by an individual hair cell, we used the conserved primers flanking splice site 3 to perform an RT-PCR analysis on isolated hair cells. Basilar papillae were dissected from chick cochleae and transected into five equal pieces. Using a different micropipette for each cell, we collected two hair cells from each region. Each pipette's content of mRNA was then independently amplified in a two-step procedure using thermostable polymerase to drive both the reverse transcription and PCR steps. The products were detected with a radiolabeled internal primer that recognized all site 3 variants. Because the two products differed only slightly in length and therefore should have been amplified with equal efficiency, the product concentrations probably reflected the relative abundances of the different mRNA species expressed in each isolated hair cell.

It was evident from this analysis that isolated hair cells

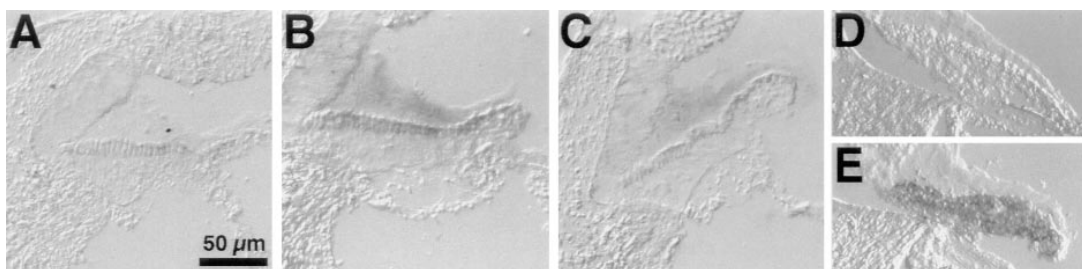


Figure 5. Localization of a *cSlo* Variant along the Embryonic Cochlea by In Situ PCR

(A–C) Expression of the SRKR insert at site 3 detected by the direct in situ RT-PCR with variant-specific primers and digoxigenin-labeled nucleotides. The cryosections were taken from the apical (A), middle (B), and basal (C) thirds of the cochlea. The labeling pattern demonstrates the selective expression of this variant in the middle third of the embryonic cochlea. Some reaction product artifactually accumulated in the tectorial membrane, the extracellular gel lying above the hair cells; in preparations of adult cochleae, this membrane generally disappeared during processing. The sections were allowed to develop for 12 hr.

(D) Primer dependency of the in situ RT-PCR product. In negative control experiments such as this, omission of the PCR primers led to negligible labeling.

(E) Localization of calbindin mRNA by the in situ RT-PCR technique. In a positive control experiment, primers designed to amplify calbindin cDNA produced strong labeling in hair and supporting cells along the entire cochlea. Only 5–10 cycles of the PCR sufficed for detection of calbindin mRNA.

express *cSlo* and that a single cell can express more than one variant. For the cells analyzed in Figure 6E, the upper bands correspond to the 4 amino acid insert SRKR, whereas the lower bands accord with the size of the insertless PCR product. The identities of these products were verified by sequencing. Interestingly, the relative intensities of the two bands varied in cells taken from different regions of the basilar papilla. The insertless variant decreased in expression from the cochlear base to the apex. The 4 amino acid variant appeared to be expressed less in the cochlea's middle region than at the apex; this variant was also absent from about half of the hair cells at the extreme cochlear base. This experiment was repeated twice; of four additional hair cells isolated from the cochlear base, two displayed the SRKR insert and two lacked it. In all three experiments, the expression pattern of the two variants exhibited with this technique accorded with that seen with the in situ RT-PCR approach: the SRKR variant is expressed at a high level in hair cells from apical regions but is barely detectable in the extreme basal hair cells; the insertless variant is expressed in hair cells throughout the epithelium, and its expression increases slightly from the cochlear apex to the base.

#### Variation in Electrophysiological Properties of K<sub>Ca</sub> Channel Isoforms

To ascertain whether the sequence differences that we observed in splice variants affect the physiological properties of the K<sub>Ca</sub> channel, we studied two *cSlo* isoforms in a heterologous expression system. Two expression constructs were fashioned in the pGW1H vector and used to transfect tsA201 cells: pGW1H-cB1 included the open reading frame for *cSlo* shown in Figure 2; pGW1H-cB2 was identical save for the absence of the SRKR insert at site 3. Macroscopic currents from inside-out membrane patches were measured under voltage-clamp conditions.

Transfection with either the pGW1H-cB1 or the pGW1H-cB2 construct resulted in a membrane current characteristic of K<sub>Ca</sub> channels. Activation of the current

was both voltage-dependent (Figure 7A) and Ca<sup>2+</sup>-sensitive (Figure 7B). As expected when the K<sup>+</sup> concentrations on both sides of a patch were equal, the current reversed at 0 mV (data not shown). The expressed channels were selectively permeable to K<sup>+</sup> over Na<sup>+</sup>: in bi-ionic experiments with Na<sup>+</sup> replacing all the K<sup>+</sup> in the solution on the patch's cytoplasmic surface, no outward current was observed at a Ca<sup>2+</sup> concentration of 1 mM for voltages as great as +160 mV (data not shown).

To minimize the complications caused by Ca<sup>2+</sup> blockage and saturation of currents at high voltage (Cox et al., 1997), we used tail current analysis to determine the channel open probability at different membrane potentials (Cui et al., 1997). To relate the probability of channel opening to the membrane potential, we then constructed a family of voltage–conductance relations that were fitted with the Boltzmann equation (Figure 7C). To ascertain the Ca<sup>2+</sup> sensitivity of the expressed channels, we fitted Ca<sup>2+</sup> concentration–conductance relations with the Hill equation (Figure 7D).

We compared the voltage dependence and the Ca<sup>2+</sup> sensitivity of cB1 and cB2 channels in three experiments. At all the Ca<sup>2+</sup> concentrations tested, cB2 channels consistently activated at more negative potentials ( $V_{1/2}$ , Figure 7E) and displayed greater voltage sensitivity ( $k$ , Figure 7G) than cB1 channels. cB2 channels also appeared to be activated at a somewhat lower Ca<sup>2+</sup> concentration ( $K_{1/2}$ , Figure 7F) and to be more Ca<sup>2+</sup>-sensitive ( $n$ , Figure 7H) than cB1 channels. Although none of the pairwise comparisons between mean values was statistically significant, the mean value of the slope parameter  $k$  for cB1 channels at all the Ca<sup>2+</sup> concentrations tested significantly exceeded that for cB2 channels by a Mann-Whitney test ( $p < 0.01$ ).

#### Discussion

To determine the molecular mechanism underlying the functional diversity of the Ca<sup>2+</sup>-activated K<sup>+</sup> channels expressed in hair cells, we have cloned and characterized cDNAs encoding K<sub>Ca</sub> channels derived from the

chicken's brain and basilar papilla. The sequence of *cSlo* cDNAs, as well as the physiological properties of heterologously expressed *cSlo* channels, indicate that the chicken's  $K_{Ca}$  channel described in this study is the ortholog of the channels cloned from the *Slowpoke* locus of *Drosophila* (Atkinson et al., 1991; Adelman et al., 1992) and the *Slo* loci of the mouse (Butler et al., 1993; Pallanck and Ganetzky, 1994) and human (Dworetzky et al., 1994; Pallanck and Ganetzky, 1994; Tseng-Crank et al., 1994; McCobb et al., 1995). The physiological properties and pattern of expression of *cSlo* are consistent with this channel's determining the electrical resonance frequencies of hair cells. Similar cDNAs have been cloned from chicken cochlear tissues by two other groups (Jiang et al., 1997; Navaratnam et al., 1997), and a partial cDNA has been characterized from the chicken's ciliary ganglion (Subramony et al., 1996).

Sequence alignments reveal that the *cSlo* primary sequence shares the hydrophobic segments reported for *dSlo*, *mSlo*, and *hSlo* channels (Atkinson et al., 1991; Butler et al., 1993; Tseng-Crank et al., 1994). Although *Slo* channels were originally thought to contain ten hydrophobic segments, an alternative topology was recently advanced on the basis of sequence alignments with voltage-activated  $K^+$  channels, functional studies, and *in vitro* translation experiments (Wallner et al., 1996). This model accommodates the presence of eleven hydrophobic segments, as observed in *cSlo*, by situating an additional transmembrane domain, now termed S3, between the original S3 and S4 segments (Atkinson et al., 1991); the erstwhile S1–S3 domains are renamed S0–S2. The S1–S6 regions of *Slo* channels are thought to share the topological arrangement and functions of their counterparts in voltage-activated ion channels (Wallner et al., 1996). The structure and roles of the four additional hydrophobic segments (S7–S10) are unknown. Based on these data and on a hydrophobicity analysis of the *cSlo* amino acid sequence, we have adopted this newly proposed topology for the *cSlo* channel structure (Figure 3A).

### Structural Heterogeneity in *cSlo* and other *Slo* Channels

*cSlo* shares a rich diversity of alternative forms with *dSlo*, *mSlo*, and *hSlo*. At the amino terminus of *cSlo*, ends of two types occur: unique termini differing in their amino acid sequences (Table 1) and truncated forms generated by the excision of intervening sequences and the recruitment of alternative translation–initiation sites (Figure 2). Both forms of sequence variability were described previously for *mSlo* (Butler et al., 1993; Pallanck and Ganetzky, 1994); published sequences (Dworetzky et al., 1994; Pallanck and Ganetzky, 1994; Tseng-Crank et al., 1994; McCobb et al., 1995) suggest that such variability occurs in *hSlo* as well. The stretch of serine residues found in the 17 amino acid variant of the *cSlo* amino terminus is common among the vertebrate *Slo* channels. The chicken's 14 amino acid amino terminus lacks this serine repeat but contains a proline repeat structure that is weakly conserved in the mouse (Butler et al., 1993).

The extensive sequence variation at the amino terminus is intriguing in light of recent evidence that this

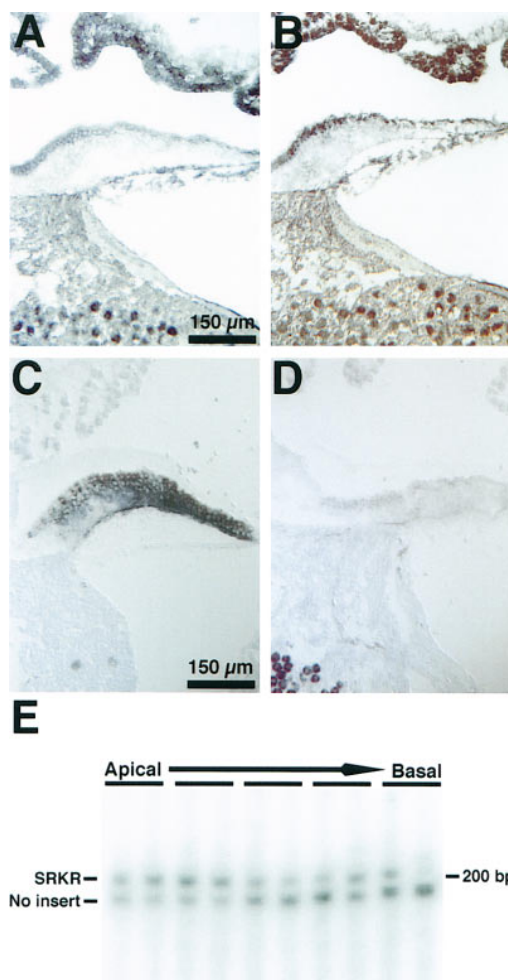


Figure 6. Localization by In Situ RT-PCR of Two Site 3 Variants in the Chick's Cochlea

(A and B) Labeling pattern of the insertless variant in apical (A) and basal (B) cochlear sections. These sections were taken from regions located 1 mm and 3 mm, respectively, from the cochlear apex. At the cochlear apex but not at the base, the expression of this variant in hair cells is reduced with respect to that in ganglion cells and tegmental cells. The sections were developed for 6 hr.

(C and D) Labeling pattern of the SRKR variant in apical (C) and basal (D) sections. These sections were taken from regions located 0.5 mm and 3.3 mm, respectively, from the cochlear apex. This variant is clearly detected in hair cells and ganglion cells but is only weakly detected in the tegmentum vasculosum. Although the labeling of hair cells is strong elsewhere, hair cells are labeled only weakly in sections from the extreme cochlear base. The sections were developed for 6 hr.

(E) RT-PCR analysis at site 3 of isolated hair cells. The basilar papilla was divided into five regions along its length. Individual hair cells were isolated from each region and analyzed by RT-PCR and Southern blotting; two cells were examined from each region. The PCR primers, identical to those used to analyze site 3 in Southern blots (Figure 3B), amplified all variants at this site. The data demonstrate that more than one variant of *cSlo* can be expressed in a single cell. The arrows indicate the predominant products expressed in these cells, which correspond to the SRKR and insertless variants. The relative abundances of the transcripts encoding each variant differ between cells, especially between those isolated from different cochlear regions. Notice that the expression of the SRKR variant is significantly diminished only in hair cells originating from the most basal region.

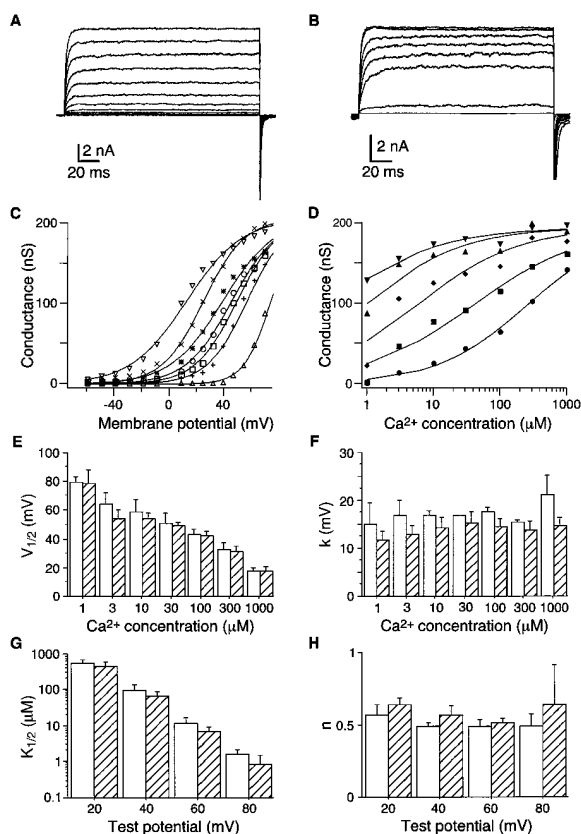


Figure 7. Electrophysiological Characterization of *cSlo* Channel Variants

(A) Current responses to test potentials from  $-60$  mV to  $+90$  mV in  $10$  mV steps. The cytoplasmic membrane surface was exposed to a free  $\text{Ca}^{2+}$  concentration of  $30 \mu\text{M}$ . This and the following three panels were derived from inside-out patch recordings of cB1 channels with symmetrical ( $144 \text{ mM}$ )  $\text{K}^+$  solutions on both sides of the membrane. The holding voltage was  $-80$  mV.

(B) Current responses to a fixed test potential of  $+60$  mV elicited in free  $\text{Ca}^{2+}$  concentrations of  $0 \mu\text{M}$ ,  $1 \mu\text{M}$ ,  $3 \mu\text{M}$ ,  $10 \mu\text{M}$ ,  $30 \mu\text{M}$ ,  $100 \mu\text{M}$ ,  $300 \mu\text{M}$ , and  $1000 \mu\text{M}$ . At the higher  $\text{Ca}^{2+}$  concentrations, channels activated rapidly and were significantly active even at the holding voltage of  $-80$  mV; the currents saturated at  $\text{Ca}^{2+}$  concentrations of  $300 \mu\text{M}$  and  $1000 \mu\text{M}$ .

(C) Conductance as a function of membrane voltage for  $\text{Ca}^{2+}$  concentrations of  $1 \mu\text{M}$  (triangles),  $3 \mu\text{M}$  (plus signs),  $10 \mu\text{M}$  (squares),  $30 \mu\text{M}$  (circles),  $100 \mu\text{M}$  (asterisks),  $300 \mu\text{M}$  ( $\times$ s), and  $1000 \mu\text{M}$  (upside-down triangles). The smooth curves show fits of each data set to a Boltzmann function,  $G = G_{\text{MAX}} / (1 + \exp[(V_{1/2} - V_m) / k])$ , in which  $G_{\text{MAX}}$ , the maximal conductance, is a free parameter obtained by fitting the data for  $1000 \mu\text{M}$   $\text{Ca}^{2+}$ . Estimates of  $V_{1/2}$  and  $k$ , which characterize a channel's voltage dependence at a given  $\text{Ca}^{2+}$  concentration, were derived from the fits.

(D) Conductance as a function of  $\text{Ca}^{2+}$  concentration at membrane test potentials of  $+20$  mV (circles),  $+40$  mV (squares),  $+60$  mV (diamonds),  $+80$  mV (triangles), and  $+100$  mV (upside-down triangles). The smooth curves demonstrate fits of each data set to the Hill equation,  $G = G_{\text{MAX}} / (1 + [(K_{1/2} / [\text{Ca}^{2+}])^n])$ . Values for  $K_{1/2}$  and the Hill coefficient  $n$ , which characterize a channel's  $\text{Ca}^{2+}$  sensitivity at a given membrane potential, were estimated from the fits.

(E-H) Summary of the values for  $V_{1/2}$  (E),  $k$  (F),  $K_{1/2}$  (G), and  $n$  (H) obtained for expression clones cB1 (open bars) and cB2 (hatched bars). Note that a lower value of  $k$  implies a higher voltage sensitivity. The uncertainties represent the SEM for three experiments with each construct.

region, along with the putative transmembrane region S0, is responsible for mediating  $\beta$  subunit regulation of  $\text{K}_{\text{Ca}}$  channels (Wallner et al., 1996). Variability in this region may be responsible for differential coupling between  $\text{K}_{\text{Ca}}$  channels and their  $\beta$  subunits or other accessory proteins. Amino-terminal variability may additionally affect the interactions among  $\text{K}_{\text{Ca}}$  channel subunits, which are thought to assemble as tetramers (reviewed in Hinrichsen, 1993). Because the region mediating the assembly of Shaker  $\text{K}^+$  channel subunits occurs at the amino terminus (Li et al., 1992; Shen et al., 1993; Babila et al., 1994), the variability of this region in *cSlo* may likewise modulate the coassembly of heteromultimers.

The only novel splice site in *cSlo* is site 2, which corresponds to the segment between the putative transmembrane domains S1 and S2 (Figure 3A). The avian sequence contains the four alternative splice sites (sites 3-6; Table 1) described for hSlo (Tseng-Crank et al., 1994); the mouse sequence also includes splice sites corresponding to *cSlo* sites 3, 4, and 6 (Butler et al., 1993; Pallanck and Ganetzky, 1994). As is the case for the human channel (Tseng-Crank et al., 1994), the 5' ends of the two exons at *cSlo* site 3 are identical, suggesting that a single exon with multiple splice sites gives rise to these variants (Table 1). A novel 59 amino acid insert at *cSlo* site 4, which was amplified only from the basilar papilla, may represent a tissue-specific variant.

The alternative 8 amino acid and 60 amino acid carboxyl termini of *cSlo* are found in hSlo and mSlo, respectively, suggesting that an alternative splice site at the carboxyl terminus is conserved. In further support of such a site, variants have also been reported at the carboxyl terminus of mSlo (Butler et al., 1993; Pallanck and Ganetzky, 1994).

In addition to the alternative splice sites discussed above, Tseng-Crank et al. (1994) described in hSlo cDNA two additional putative splice sites located upstream of a site corresponding to *cSlo* site 3. Navaratnam et al. (1997) describe still another splice site between the S6 and S7 domains. Taken together, the various sources suggest the existence of as many as ten alternative splice sites in the Slo channels of vertebrates. Because most of these sites occur in both avian and mammalian channels, the alternative splice sites may be conserved throughout the higher vertebrates.

Several of the splice variants contain consensus sequences for phosphorylation by protein kinases (Table 1) (Pinna and Ruzzene, 1996). The 8 amino acid insert at *cSlo* site 2 contains such a site; if the newly proposed Slo topology is correct, however, this novel insert occurs in an extracellular loop. Although it remains to be determined whether the variants with potential phosphorylation sites are regulated by intracellular signaling,  $\text{K}_{\text{Ca}}$  channels are known to be directly modulated by G proteins, protein kinases and phosphatases, cyclic nucleotides, fatty acids, and lipids (reviewed in Hinrichsen, 1993). The conservation of both exon variants and potential phosphorylation sites suggests that these variants play important roles in modulating the properties of Slo channels.

#### Expression Pattern of *cSlo* and Its Variants in the Chicken's Cochlea

Using single-cell and in situ RT-PCR analyses, we have localized *cSlo* expression to hair cells distributed along

the entire length of the basilar papilla. Although physiological studies did not detect these channels in hair cells originating from the extreme apex of the basilar papilla (Fuchs and Evans, 1990), the present results suggest that these channels are more widely distributed. The expression pattern suggests that  $K_{Ca}$  channels play a role in electrical frequency tuning over the 50–5000 Hz range of the chicken's cochlea (Gray and Rubel, 1985). Extensive modulation of  $K_{Ca}$  channel kinetics must be necessary to account for tuning throughout this range.

The expression of *cSlo* in the tegmentum vasculosum was not unexpected. Maxi-K channels are expressed in marginal cells of the stria vascularis (Takeuchi et al., 1992), the analog of the chicken's tegmentum vasculosum (Manley, 1990). Like the stria, the tegmentum is likely to be responsible for producing the high  $K^+$  endolymph that bathes the apical surfaces of hair cells. *cSlo* channels could be involved in  $Ca^{2+}$ -dependent secretion of  $K^+$  into the cochlear duct or in the establishment of the electrochemical gradient necessary to drive  $K^+$  secretion.

Using the single-cell and in situ RT-PCR techniques, we have localized the expression of two *cSlo* splice variants in the cochlea. Both the insertless and 4 amino acid variants at site 3 are expressed in hair cells and ganglion cells, whereas the insertless variant alone occurs in the tegmentum vasculosum. The insertless variant is expressed in hair cells along the entirety of the papilla, but the 4 amino acid variant is excluded from the extreme base. The data indicate that at least some splice variants are restricted to discrete regions of the basilar papilla. These results furthermore suggest that a distinct spatial pattern of alternative splicing of *cSlo* mRNA helps determine the tonotopic map of the cochlea.

There was an intriguing discrepancy between the expression pattern of the SRKR variant at site 3 in the embryonic cochlea and that of the chick. In the former, the variant was found only in hair cells localized to the middle third of the basilar papilla. In the chick's cochlea, however, the 4 amino acid insert was distributed along most of the papilla and was excluded only from the extreme base of the organ. This developmental change in the expression pattern of *cSlo* variants may reflect the shift in response frequency during cochlear ontogeny (Rubel, 1984; Rubel et al., 1984; reviewed in Manley, 1996). Alternatively, the change may represent the acquisition of  $K_{Ca}$  currents at a time during embryogenesis when auditory function matures rapidly (Fuchs and Sokolowski, 1990).

#### Extensive Alternative Splicing of *cSlo* mRNA and Hair-Cell Diversity

If all of the potential alternative splice sites of *Slo* channels occur in the chicken, and if alternative exons occur at each site, then the possible number of distinct  $K_{Ca}$  channels greatly exceeds the 576 implied by our study. This degree of diversity exceeds that reported for other alternatively spliced channels. Such an immense variability is not surprising, however, in light of the widespread distribution and functional heterogeneity of  $K_{Ca}$  channels (reviewed in Latorre et al., 1989; Hinrichsen, 1993).

A major goal of research in this area is to relate the isoforms of *Slo* channels to their specific functions. The physiological properties of some splice variants have been described for *Drosophila* (Adelman et al., 1992; Lagrutta et al., 1994) and human channels (Tseng-Crank et al., 1994). Variants with differential sensitivity to  $Ca^{2+}$  have been reported for both species, and several splice sites affecting channel gating, channel kinetics, and single-channel conductance were found in *Drosophila*. Modulation of all of these physiological properties could affect the electrical resonance of hair cells and thus adjust their characteristic frequencies (Hudspeth and Lewis, 1988b).

Our physiological recordings have confirmed that *cSlo* cDNA encodes a  $Ca^{2+}$ -activated  $K^+$  channel (Jiang et al., 1997). Moreover, it is heartening that *cSlo* channels with and without the SRKR insert at splice site 3 differ significantly in their voltage sensitivities and may vary as well in their ranges of activation by  $Ca^{2+}$  and by voltage. At present, however, there are three reasons that it would be premature to relate the properties of heterologously expressed channels to the electrical resonance frequencies of hair cells in which similar channels are expressed. First, the heterologously expressed *cSlo* channels clearly differ from native channels. Most strikingly, the membrane potential at which the channels are half activated at a  $Ca^{2+}$  concentration of 100  $\mu$ M is nearly 70 mV more positive in the expressed than in native channels (Roberts et al., 1990). This abnormality, which has been observed in other heterologously expressed *Slo* channels, may result from the absence of  $\beta$  subunits (McManus et al., 1995). The second reservation is that cB1 and cB2 channels might not represent naturally occurring isoforms. Because the two expression constructs were assembled from three cDNA fragments, each of which included at least one splice site with a particular variant, the products might have combined exons that do not naturally occur together and might thereby have produced channels with aberrant physiological properties. Finally, the heterologous expression of a pure population of channel subunits excludes the possible formation of heteromultimers (Wu and Fettiplace, 1996), whose properties may influence channel kinetics.

It has been speculated that the admixture of a few  $K_{Ca}$  channel subunits into heterotetramers with physiological properties intermediate between those of the homotetramers accounts for variable frequency tuning in the turtle's basilar papilla (Wu and Fettiplace, 1996). Heteromultimer assembly may provide an additional mechanism of variability in the chicken's papilla as well. Indeed, our single-cell RT-PCR analysis shows that an individual hair cell can express more than one type of subunit. Because the frequency range of the chicken exceeds that of the turtle, a greater number of distinct subunits may be necessary to establish the latter's tonotopic map. Considering then the wealth of splice variants, the potential for heterotetramer formation, and the possibility of differential modulation by  $\beta$  subunits, the full spectrum of possible channel properties, and thus of hair-cell phenotypes, is vast.

The range of  $K_{Ca}$  channel expression in the chicken's cochlea is but one manifestation of the remarkable diversity of hair cells in this organ. Along the basilar papilla,

there are systematic variations in the expression of delayed rectifier and inward rectifier K<sup>+</sup> channels (Fuchs and Evans, 1990; Navaratnam et al., 1995). Moreover, the numbers of these channels and of A-type, SK, and acetylcholine receptor channels vary across the cochlea, from tall hair cells to short (Murrow and Fuchs, 1990; Murrow, 1994; reviewed in Fuchs, 1992, 1996). In conjunction with the gradations in cell body and hair bundle morphology along and across the basilar papilla (Figure 1) (Tilney et al., 1992), these systematic variations in the complement of ion channels imply that the chicken's cochlea contains 10,000 hair cells with 10,000 different phenotypes! By revealing the wealth of cSlo variants, the present study sets the stage for a systematic molecular analysis of the complex expression pattern of ion channels in the cochlea.

#### Experimental Procedures

All of the experiments in the present paper were performed on chickens (*Gallus gallus*) of the White Leghorn strain. Animals were investigated at two stages: embryos in their seventeenth through nineteenth days of incubation (E16–E18) and chicks 1–2 weeks of age.

#### Isolation of cSlo cDNAs

Using the Pileup program (Genetics Computer Group, Madison, WI) on the homologous sequences *dSlo* (Atkinson et al., 1991), *mSlo* (Butler et al., 1993), and *hSlo* (Tseng-Crank et al., 1994), we designed six degenerate primers (all sequences are given in a 5'-to-3' orientation): S1 forward, GTNCAYGARCCYAARATG; pore forward, ACGTNGGNTAYGGNGAYGT; S8 forward, ATGATHGCNATHGARTAYAA; S7 reverse, YTGIGCDATRAANCCNAR; S7–S8 reverse, YTCNGTRTACATYTCRTT; and S10 reverse, ATRCANTADTGNTTRGG. These were used in PCRs with poly(dT)<sub>18</sub>-primed cDNA reverse transcribed from 1 µg of chicken brain polyadenylated mRNA. Hot start PCRs were initiated by adding *Taq* polymerase (Promega, Madison, WI) at 94°C, followed by 40 cycles of 94°C for 1 min, 45°C for 1 min, and 72°C for 1 min, with a final extension for 5 min at 72°C.

The PCR products were gel purified, subcloned (pCRII, Invitrogen, Carlsbad, CA), and sequenced. Clones that contained K<sub>ca</sub> channel sequences were used as probes to screen a chicken brain cDNA library (5'-STRETCH, Clontech Laboratories, Inc., Palo Alto, CA) by plaque hybridization. The inserts of eight positive clones were subcloned into the pBluescript II SK (+) vector (Stratagene, La Jolla, CA) and fully sequenced on both DNA strands.

Using a 5' end, 1.5 kbp PCR product as probe, we additionally screened a cDNA library constructed in the HybriZAP vector (Stratagene) from the basilar papillae of late embryonic chickens. cDNA inserts were isolated by *in vivo* excision with helper bacteriophage (ExAssist, Stratagene) and sequenced in both directions.

Sequences were analyzed with the programs Sequencher (Gene Codes Corp., Ann Arbor, MI), AIIAII (Computational Biochemistry Research Group, Institute for Scientific Computing, Zürich, Switzerland), MacDNASIS (Hitachi Software, San Bruno, CA), GCG (Genetics Computer Group), and Lasergene (DNASTar, Madison, WI).

#### Detection of cSlo Splice Variants by RT-PCR Analysis

Cochleae were dissected from chicks and placed in low divalent cation medium (Zidanic and Fuchs, 1995). The tegmentum vasculosum was isolated, the basilar papilla was scraped from the underlying basilar membrane with a tungsten needle, and both samples were frozen in liquid nitrogen. Total RNA was isolated from papillae and tegmenta by acid-phenol extraction (Chomczynski and Sacchi, 1987). The RNA from the equivalent of a single papilla or tegmentum was used to synthesize cDNA with reverse transcriptase (Superscript II, Life Technologies, Grand Island, NY) and poly(dT)<sub>18</sub> primers. Total RNA isolated from the chicken's brain was used for comparison and as a control for the PCRs.

To amplify alternative exons, we used the following PCR primers:

site 2 forward, AGGAGAACGTGGCAGCAGAAG, site 2 reverse, TGAAACGCAAGCCGAAGTAGAG; site 3 forward, ATGATAGCCATA GAATACAAGTCGG, site 3 reverse, CCACACTTTTTATCCTTTT GGG; site 4 forward, ACCTTAGGATTCTTCATTGCAAGTG, site 4 reverse, GTGAGGAGTTGGGTGAATTTCC; site 5 forward, ATGGAG GCATGCGAAATTCACC; site 5 reverse, TCATCGCTGCTTCACTTCG AGT; site 6 forward, GGACAAGGAATGCATCTTGG; and site 6 reverse, GCAAATGGCCCATCATACAAAG. Hot start PCRs were initiated as described above, followed by 30–35 cycles of 94°C for 1 min, 52–57°C for 1 min, and 72°C for 1 min, with a final extension at 72°C for 5 min. cDNA was synthesized with the total RNA isolated from one to ten basilar papillae; a tenth of the cDNA generated from a single papilla served as the template for each PCR.

To characterize the variants expressed at sites 1 and 7, we employed the RACE technique (Marathon, Clontech) to amplify the 5' and 3' termini of *cSlo* mRNAs from the total RNA of ten basilar papillae. Designed to anneal within a few hundred base pairs of sites 1 and 7, the forward and reverse primers were: site 1 reverse, GGCTCCTTGTTTTGACC and site 7 forward, TCCATCCCATCAA CAGCAA. The PCR entailed 30–35 cycles of 94°C for 1 min, 58°C for 1 min, and 72°C for 1 min, with a final extension at 72°C for 5 min. The products were purified, subcloned, and sequenced.

Sites 1 and 7 were additionally screened by PCR analysis of the chicken cochlear library. To amplify the 5' and 3' ends of the library clones, the forward and reverse primers described above were paired with HybriZAP (Stratagene) vector primers that flanked the cDNA inserts. The library clones were amplified under the PCR conditions described above.

To analyze the alternative exons expressed at each site, we resolved the PCR products on 2% agarose gels (Metaphor, FMC Bio-Products, Rockland, ME); products visualized by ethidium bromide staining were verified by subcloning and sequencing.

Southern blots were analyzed by hybridization at 50°C with an end labeled oligonucleotide probe, GGCATTTTTACTGCAAGGCC, designed to recognize a conserved region just upstream of splice site 3. The blots were hybridized for 3 hr and washed for 10 min in 4× SSC and 0.1% (v/v) sodium dodecyl sulfate (SDS) at 37°C and for 20 min in 2× SSC and 0.1% (v/v) SDS at 37°C; 1× SSC contains 150 mM NaCl and 15 mM sodium citrate (pH 7.0). The blots were then analyzed on a phosphor scanner (Molecular Dynamics, Sunnyvale, CA).

#### Northern Analysis

Total RNA was isolated from chicken brains, eyes, and cochleae by acid-phenol extraction. Five micrograms of total RNA from each tissue was size fractionated on a 1% formaldehyde-agarose gel, transferred to a nylon membrane (Micron Separations, Inc., Westborough, MA), and immobilized by baking at 80°C for 2 hr. A 3.6 kbp DNA fragment containing the entire coding sequence of *cSlo* was used to probe membranes at 68°C (ExpressHyb, Clontech). The blots were washed in 2× SSC and 0.05% (v/v) SDS three times for 10 min each at 50°C and in 0.1× SSC and 0.1% (v/v) SDS twice for 20 min each at 50°C, then exposed for 1 week to film (X-Omat, Kodak, New Haven, CT).

#### In Situ Hybridization

Temporal bones were dissected from embryonic cochleae and fixed overnight at 4°C in 4% (w/v) paraformaldehyde and PBS (150 mM NaCl, 3 mM KCl, 8 mM Na<sub>2</sub>HPO<sub>4</sub>, and 2 mM KH<sub>2</sub>PO<sub>4</sub> [pH 7.4]). The specimens were washed in PBS, cryoprotected with 30% (w/v) sucrose in PBS, and embedded (Tissuetek, Miles Inc., Elkhart, IN). Digoxigenin-labeled antisense RNA probes were transcribed (DIG RNA-labeling kit, Boehringer Mannheim) from a *cSlo* fragment comprising nucleotides 2148–2973 (Figure 2). In situ hybridization was conducted (Strähle et al., 1994) on 14 µm cryosections with 100 µl of diluted probe (1:100) in hybridization buffer. After incubation overnight at 65°C in a chamber humidified with 50% (v/v) formamide and 1× SSC, sections were washed twice for 15 min each at 65°C in 50% (v/v) formamide and 2× SSC. The slides were next washed twice for 30 min each at 65°C in 25% (v/v) formamide, 1× SSC, and half-strength PBS and transferred to PBS for 5 min at room temperature.

For antibody detection, sections were blocked for 1 hr in PBS,

0.3% (w/v) BSA, 0.5% (w/v) Blocking Reagent (Boehringer Mannheim, Indianapolis, IN), and 0.1% (v/v) polyoxyethylene-20-sorbitan monolaurate (Tween 20, Fisher Scientific, Fair Lawn, NJ). Sections were incubated for 2 hr at room temperature with anti-digoxigenin Fab-alkaline phosphatase conjugate (Boehringer Mannheim) at a dilution of 1:1500 in the solution above. Unbound Fab fragments were removed by washing four times for 20 min each in PBS with 1% (v/v) Tween 20 and twice for 20 min each in PBS. For detection, the sections were preincubated for 20 min in 100 mM NaCl, 50 mM MgCl<sub>2</sub>, and 100 mM Tris-HCl (pH 9.5), then incubated for 48 hr in this solution with 0.34 mg/ml nitroblue tetrazolium salt and 0.175 mg/ml 5-bromo-4-chloro-3-indolyl-phosphate (5 Prime→3 Prime, Inc.). The color reaction was stopped with 2 mM EDTA in PBS and the slides were mounted in 50% (v/v) glycerol in PBS. Photographs were taken on slide film (Ektachrome 160T, Kodak) with an Axiovert 135 microscope and MC80 camera (Carl Zeiss, Jena, Germany).

#### In Situ RT-PCR Analysis of Cochlear Frozen Sections

In the in situ PCR procedure, three labeling techniques were used to detect *cSlo* products in embryonic and hatchling cochleae. First, to detect *cSlo* mRNA in the embryonic cochlea and retina, 5' end-labeled primers were directly incorporated during amplification. In the second technique, the SRKR variant was labeled in the embryonic cochlea by incorporation of digoxigenin-labeled nucleotides into the PCR products. Finally, the PCR products produced in the chick's cochlea were detected by hybridization with digoxigenin-conjugated probes.

Temporal bones were removed from chicks and fixed for 18–24 hr at 4°C in 4% (w/v) paraformaldehyde, 77 mM Na<sub>2</sub>HPO<sub>4</sub>, and 23 mM NaH<sub>2</sub>PO<sub>4</sub> (pH 7.4). The specimens were then dehydrated and demineralized over a period of 1 week in several changes of 50 mM EDTA and 30% (w/v) sucrose in PBS. After embedment, 8–10 mm frozen sections were cut and applied to pretreated microscope slides (Superfrost+, MJ Research, Watertown, MA). To stabilize sections on the slides, they were heat treated at 105°C for 30 s (Bagasra and Hansen, 1997), then postfixed for 2 hr at room temperature with 2% (w/v) paraformaldehyde in PBS. To facilitate the permeation of reagents, the sections were digested for 5 min at room temperature with 0.5 µg/ml proteinase K in 5 mM EDTA and 100 mM Tris-HCl (pH 7.5). Nuclear DNA was degraded by incubating the sections overnight with 1000 unit/ml deoxyribonuclease I (Boehringer Mannheim) in 50 mM KCl, 2 mM MgCl<sub>2</sub>, and 20 mM Tris-HCl (pH 8.4). The sections were washed in 2 mM EDTA and 20 mM Tris-HCl (pH 7.5) to remove the deoxyribonuclease then dehydrated through a graded ethanol series and air dried.

The RT and PCR steps were conducted under a single coverslip with the SuperScript II One-Step RT-PCR system (Life Technologies). The reaction solution included 1 µM of forward and reverse primers, 2 µl of Superscript II RT/*Taq* mixture, and 2.5 mM MgSO<sub>4</sub>. The variant-specific primers used for the amplification of the insertless and SRKR inserts were: insertless forward, CACCAGGCTT TCAACAATG; insertless reverse, TGATCAATATACTGCTTTCTCTTT; SRKR forward, ATGATAGCATAGAATACAAGTCGG; and SRKR reverse, CCACACTTTTTATCCTTTTGGG. For thermal cycling of the microscope slides, we employed the PTC-200 DNA Engine fitted with the Twin Tower Block (MJ Research). Reverse transcription was initiated by heating slides to 50°C before application of the reaction mixture. After an initial incubation at 50°C for 30 min to effect reverse transcription, 30 cycles were performed at 92°C for 20 s, 55°C for 15 s, and 72°C for 45 s, with a final extension of 5 min at 72°C.

After amplification, coverslips were removed by soaking slides for 5 min in 2× SSC at room temperature. The slides were then washed twice for 5 min each at room temperature in 2× SSC and dehydrated in a graded ethanol series. PCR products were labeled by hybridization at 37°C with 500 ng/ml digoxigenin-labeled oligo-probe (GGCATTCTTTACTGCAAGGCC for the insertless variant or AATATACGCTTTTCGGCTTCTGCT for the SRKR variant) in 100 µl of a hybridization solution comprising 2× SSC, 50% (v/v) formamide, 10 mg/ml sheared herring sperm DNA, 1% (v/v) SDS, and 10× Denhardt's solution (5 Prime→3 Prime). After incubation for 18 hr at 37°C under coverslips, the sections were washed once for 10 min at room temperature in 2× SSC to remove the coverslips. The slides

were then washed twice for 10 min each at 37°C in 2× SSC, twice for 10 min each at 37°C in 1× SSC, twice for 5 min each at 37°C in 0.2× SSC, and finally once at room temperature for 10 min in 200 mM NaCl, 3 mM KCl, and 50 mM Tris-HCl (pH 7.5).

For detection of the digoxigenin-labeled probes, the sections were blocked for 20 min in 2% (w/v) Blocking Reagent (Boehringer Mannheim), 3% (w/v) bovine serum albumin, 100 mM NaCl, 2 mM MgCl<sub>2</sub>, and 100 mM Tris-HCl (pH 7.5). The sections were subsequently incubated for 2 hr at room temperature with anti-digoxigenin Fab-alkaline phosphatase conjugate at a dilution of 1:1500 in the blocking solution above. Unbound fragments were removed by washing four times for 20 min each in 0.025% (v/v) Tween 20, 100 mM NaCl, 2 mM MgCl<sub>2</sub>, and 100 mM Tris-HCl (pH 7.5), and twice for 30 min each in this solution without the detergent. Alkaline phosphatase development was undertaken as described for the in situ hybridizations.

For the detection of *cSlo* mRNA in the embryonic retina and cochlea (Figures 4B and 4C), the same procedure was used except that the RT-PCR primers were synthesized with digoxigenin labels at their 5' ends for direct incorporation into the amplification products. Hybridization with an internal oligonucleotide probe was accordingly omitted. After amplification, excess primer was removed by washing the sections twice for 20 min each at 47°C in 0.1× SSC. For detection of the SRKR variant in the embryonic cochlea (Figure 5), we used this procedure except that the thermostable polymerase *rTth* was employed in the RT and PCR steps (EZ Kit, Perkin Elmer). Digoxigenin-labeled dUTP (Boehringer Mannheim) was directly incorporated into the PCR products.

We found that the indirect detection method was most useful for estimating the relative expressions of exon variants. The two direct methods were more sensitive, however, and the labeled PCR primers consistently yielded the lowest background levels.

To avoid variability in labeling patterns due to differences in treatment at any stage, apical and basal cochlear sections were attached to the same slides, received identical treatment before amplification, and underwent the amplification steps under a common coverslip.

#### Single-Cell RT-PCR Analysis of Isolated Hair Cells

A chick's papilla was cut into five equal segments along its length with a fine tungsten needle. Each segment was digested for 15–20 min with 0.1 mg/ml papain (Worthington Biochemical Corp., Freehold, NJ) in 2.5 mM cysteine hydrochloride, 1 mM EGTA, 1 mM MgCl<sub>2</sub>, and PBS. The segments were then washed several times with PBS to remove protease. Single cells were dissociated by trituration of the epithelium with a microelectrode pulled to a tip diameter of 100–200 µm. An additional micropipette with a tip diameter of 10–30 µm was utilized to pick up each isolated cell to be studied. The movement of a cell into the micropipette was controlled by negative pressure; the capture of an individual cell was clearly visible under an inverted microscope. The contents of each micropipette were dispensed into a 0.65 ml tube by breaking the tip inside the tube and centrifugation. The RT and PCR steps were carried out in the same tube with thermostable *rTth* reverse transcriptase (RNA PCR Kit, Perkin Elmer). To amplify the alternative exons expressed at site 3 in single cells, we used the primers and thermal cycler conditions described for the RT-PCR characterization of site 3. Southern blots of the PCR products were analyzed as described.

#### Heterologous Expression and Electrophysiology

To express *cSlo* channels, we initially assembled an expression construct comprising the open reading frame shown in Figure 2, together with 5' and 3' untranslated regions of approximately 400 bp and 40 bp, respectively. After transfection in the vector pBKCMV (Stratagene), the construct produced only small and erratic currents when expressed in HEK 293 cells. We subsequently deleted approximately 360 bp of the 5' untranslated region and subcloned the product in the pGW1H vector (British Biotech, Oxford, UK), which contains 1805 bp of the human cytomegalovirus promoter sequence. The resultant construct was termed pGW1H-cB1. A second expression construct, pGW1H-cB2, was created by removal of the 12 bp encoding the SRKR insert at site 3.

We used liposome-mediated transfection (LipofectAMINE, Life Technologies, Gaithersburg, MD) to transiently transfect tsA201 cells,

which are HEK 293 cells stably transfected with large T antigen (Margolske et al., 1993). The Slo constructs were expressed in conjunction with a plasmid ( $\pi$ H3 CD8) expressing human lymphocyte CD8, which served as a reporter molecule. Betrayed by their binding of anti-CD8 antibody-coated beads (Dynal, Great Neck, NY), transfected cells were studied 12–72 hr later. The combination of the shortened 5' untranslated region, a potent promoter, and the T antigen greatly increased the channels' expression. At a potential of +80 mV and in the presence of 30  $\mu$ M Ca<sup>2+</sup>, for example, inside-out patches from tsA201 cells transfected with the pGW1H-cB1 construct often displayed K<sup>+</sup> currents exceeding 10 nA. The expression levels of the two constructs were comparable. In the absence of transfection, tsA201 cells displayed negligible ionic current.

To investigate the channels' Ca<sup>2+</sup> sensitivity and voltage dependency, we performed recordings in the inside-out patch-clamp configuration. Electrodes with series resistances of 1–3 M $\Omega$  were pulled from borosilicate glass (Drummond Scientific, Broomall, PA). Each pipette's taper was coated with beeswax; the tip was fire polished before use.

The recording pipettes contained 144 mM K<sup>+</sup>, 1.5 mM Mg<sup>2+</sup>, 143 mM Cl<sup>-</sup>, 0.5 mM EGTA, and 5 mM HEPES (pH 7.2). The cytoplasmic surface of a membrane patch was superfused with a bath solution containing 144 mM K<sup>+</sup>, 140 mM Cl<sup>-</sup>, 0.5 mM EGTA, 5 mM HEPES (pH 7.2), and an amount of CaCl<sub>2</sub> appropriate to generate a defined free Ca<sup>2+</sup> concentration. Ultrapure chemicals (Aldrich Chemical Co., Inc., Milwaukee, WI; Sigma Chemical Co., St. Louis, MO) were used to minimize the effects of contaminating divalent cations on the channels' activity (Cox et al., 1997). We used a program (Shuster et al., 1991) to calculate the amount of CaCl<sub>2</sub> needed to achieve free Ca<sup>2+</sup> concentration of 1–1000  $\mu$ M. The concentration of free Ca<sup>2+</sup> was confirmed with a Ca<sup>2+</sup>-sensitive electrode (Orion Research Inc., Boston, MA). Dithiothreitol was added to the bath solution at a concentration of 1 mM to prevent channel deterioration due to oxidation (DiChiara and Reinhart, 1997; Wang et al., 1997). An agar bridge was used to protect the silver–silver chloride ground wire from reacting with dithiothreitol.

Currents were recorded with an EPC-7 amplifier (List-Electronic, Darmstadt, Germany), low pass filtered at 4 kHz with an 8-pole Bessel filter, and stored on tapes (VR-10B digital data recorder, Instrutech Instruments, Great Neck, NY; SLV420, Sony, Tokyo, Japan). Current responses to voltage pulses were additionally digitized at 20 kHz, averaged, and recorded with an analog-to-digital converter linked by a direct memory access unit to a computer (Quadra 800, Apple Computer, Cupertino, CA) running LabView software (version 3.1, National Instruments, Inc., Austin, TX).

Because of the large current traversing the electrode in some experiments, the voltage drop due to the electrode's resistance could contribute a voltage error as great as 30 mV. To construct accurate current–voltage relations, we therefore compensated the membrane voltage before further data analysis. Data were analyzed with statistical (StatView, Abacus Concepts, Berkeley, CA) and curve-fitting software (Igor Pro, WaveMetrics Inc., Lake Oswego, OR) with a Levenberg-Marquardt algorithm for nonlinear least square fits.

The two parameters necessary to fit conductance–voltage relations to the Boltzmann equation,  $V_{1/2}$  and  $k$ , characterize a channel's voltage dependence.  $V_{1/2}$  is defined as the voltage at which the conductance attains half its maximal value at a particular Ca<sup>2+</sup> concentration. The slope factor  $k$ , the voltage change required for an e-fold change of the channel's open probability, represents the steepness of a channel's voltage sensitivity. Fits of concentration–conductance relations with the Hill equation provide estimates of two additional parameter values,  $K_{1/2}$  and  $n$ , which reflect a channel's Ca<sup>2+</sup> sensitivity.  $K_{1/2}$  is the concentration of Ca<sup>2+</sup> at which the conductance reaches half its maximal value at a given voltage;  $n$  is the Hill coefficient, which reflects the cooperativity of Ca<sup>2+</sup> binding associated with channel activation.

#### Acknowledgments

The authors thank Ms. R. Pironkova for outstanding technical assistance, Mr. C. McKinney for computer programming, Dr. G. Yellen for helpful suggestions about channel expression, Dr. J. C. Oberholzer and his colleagues for access to data prior to publication, Dr.

R. Horn for the use of tsA201 cells, Dr. C. Miller for access to the  $\pi$ H3 CD8 plasmid, and Dr. G. Roberts of British Biotech Pharmaceuticals Limited for the use of the pGW1H expression vector. The members of our research group, particularly the estimable Ms. E. A. Lumpkin and Drs. J. L. Cyr and R. J. E. Kollmar, made valuable comments on the manuscript. This work was begun at University of Texas Southwestern Medical Center, where K. P. R. was supported by National Institutes of Health grant GM08014 and the Perot Family Foundation. This research was supported by grant DC00317 from the National Institutes of Health. Z.-P. S. and S. H. are Associates and A. J. H. is an Investigator of the Howard Hughes Medical Institute.

Received September 24, 1997; revised October 24, 1997.

#### References

- Adelman, J.P., Shen, K.-Z., Kavanaugh, M.P., Warren, R.A., Wu, Y.-N., Lagrutta, A., Bond, C.T., and North, R.A. (1992). Calcium-activated potassium channels expressed from complementary DNAs. *Neuron* 9, 209–216.
- Art, J.J., and Fettiplace, R. (1987). Variation of membrane properties in hair cells isolated from the turtle cochlea. *J. Physiol.* 385, 207–242.
- Art, J.J., Wu, Y.-C., and Fettiplace, R. (1995). The calcium-activated potassium channels of turtle hair cells. *J. Gen. Physiol.* 105, 49–72.
- Ashmore, J.F. (1983). Frequency tuning in a frog vestibular organ. *Nature* 304, 536–538.
- Atkinson, N.S., Robertson, G.A., and Ganetzky, B. (1991). A component of calcium-activated potassium channels encoded by the *Drosophila slo* locus. *Science* 253, 551–555.
- Babila, T., Moscucci, A., Wang, H., Weaver, F.E., and Koren, G. (1994). Assembly of mammalian voltage-gated potassium channels: evidence for an important role of the first transmembrane segment. *Neuron* 12, 615–626.
- Bagasra, O., and Hansen, J. (1997). In situ PCR: DNA and RNA targets. In *In Situ PCR Techniques* (New York: John Wiley and Sons, Inc.), pp. 37–60.
- Butler, A., Tsunoda, S., McCobb, D.P., Wei, A., and Salkoff, L. (1993). *mSlo*, a complex mouse gene encoding "Maxi" calcium-activated potassium channels. *Science* 261, 221–224.
- Chen, L., Salvi, R., and Shero, M. (1994). Cochlear frequency-place map in adult chickens: intracellular biocytin labeling. *Hear. Res.* 81, 130–136.
- Chomczynski, P., and Sacchi, N. (1987). Single-step method of RNA isolation by acid guanidinium thiocyanate-phenol-chloroform extraction. *Anal. Biochem.* 162, 156–159.
- Cox, D.H., Cui, J., and Aldrich, R.W. (1997). Separation of gating properties from permeation and block in *mslo* large conductance Ca-activated K<sup>+</sup> channels. *J. Gen. Physiol.* 109, 633–646.
- Crawford, A.C., and Fettiplace, R. (1980). The frequency selectivity of auditory nerve fibres and hair cells in the cochlea of the turtle. *J. Physiol.* 306, 79–125.
- Crawford, A.C., and Fettiplace, R. (1981). An electrical tuning mechanism in turtle cochlear hair cells. *J. Physiol.* 312, 377–412.
- Cui, J., Cox, D.H., and Aldrich, R.W. (1997). Intrinsic voltage dependence and Ca<sup>2+</sup> regulation of *mslo* large conductance Ca-activated K<sup>+</sup> channels. *J. Gen. Physiol.* 109, 647–673.
- DiChiara, T.J., and Reinhart, P.H. (1997). Redox modulation of *hslO* Ca<sup>2+</sup>-activated K<sup>+</sup> channels. *J. Neurosci.* 17, 4942–4955.
- Dworetzky, S.I., Trojnacki, J.T., and Gribkoff, V.K. (1994). Cloning and expression of a human large-conductance calcium-activated potassium channel. *Mol. Brain Res.* 27, 189–193.
- Freeman, D.M., and Weiss, T.F. (1990). Superposition of hydrodynamic forces on a hair bundle. *Hear. Res.* 48, 1–16.
- Frishkopf, L.S., and DeRosier, D.J. (1983). Mechanical tuning of free-standing stereociliary bundles and frequency analysis in the alligator lizard cochlea. *Hear. Res.* 12, 393–404.
- Frohman, M.A. (1993). Rapid amplification of complementary DNA

- ends for generation of full-length complementary cDNAs: thermal RACE. *Methods Enzymol.* **218**, 340–358.
- Fuchs, P.A. (1992). Ionic currents in cochlear hair cells. *Prog. Neurobiol.* **39**, 493–505.
- Fuchs, P.A. (1996). Synaptic transmission at vertebrate hair cells. *Curr. Opin. Neurobiol.* **6**, 514–519.
- Fuchs, P.A., and Evans, M.G. (1988). Voltage oscillations and ionic conductances in hair cells isolated from the alligator cochlea. *J. Comp. Physiol. A* **164**, 151–163.
- Fuchs, P.A., and Evans, M.G. (1990). Potassium currents in hair cells isolated from the cochlea of the chick. *J. Physiol.* **429**, 529–551.
- Fuchs, P.A., and Sokolowski, B.H.A. (1990). The acquisition during development of Ca-activated potassium currents by cochlear hair cells of the chick. *Proc. R. Soc. Lond. B* **241**, 122–126.
- Fuchs, P.A., Nagai, T., and Evans, M.G. (1986). Electrical tuning in hair cells isolated from the chick cochlea. *J. Neurosci.* **8**, 2460–2467.
- Fuchs, P.A., Evans, M.G., and Murrow, B.W. (1990). Calcium currents in hair cells isolated from the cochlea of the chick. *J. Physiol.* **429**, 553–568.
- Gray, L., and Rubel, E.W. (1985). Development of absolute thresholds in chickens. *J. Acoust. Soc. Am.* **77**, 1162–1172.
- Gummer, A.W., Smolders, J.W., and Klinke, R. (1987). Basilar membrane motion in the pigeon measured with the Mössbauer technique. *Hear. Res.* **29**, 63–92.
- Hinrichsen, R.D. (1993). Ca<sup>2+</sup>-dependent K<sup>+</sup> channels: distribution and function. In *Calcium-Dependent Potassium Channels*, R.D. Hinrichsen, ed. (Austin: R. G. Landes), pp. 16–31.
- Hirokawa, N. (1978). The ultrastructure of the basilar papilla of the chick. *J. Comp. Neurol.* **181**, 361–374.
- Holton, T., and Hudspeth, A.J. (1983). A micromechanical contribution to cochlear tuning and tonotopic organization. *Science* **222**, 508–510.
- Hudspeth, A.J. (1989). How the ear's works work. *Nature* **341**, 397–404.
- Hudspeth, A.J., and Lewis, R.S. (1988a). Kinetic analysis of voltage- and ion-dependent conductances in saccular hair cells of the bullfrog, *Rana catesbeiana*. *J. Physiol.* **400**, 237–274.
- Hudspeth, A.J., and Lewis, R.S. (1988b). A model for electrical resonance and frequency tuning in saccular hair cells of the bullfrog, *Rana catesbeiana*. *J. Physiol.* **400**, 275–297.
- Jiang, G.-J., Zidanic, M., Michaels, R.L., Michael, T.H., Griguer, C., and Fuchs, P.A. (1997). *cSlo* encodes calcium-activated potassium channels in the chick's cochlea. *Proc. R. Soc. Lond.* **264**, 731–737.
- Jones, S.M., and Jones, T.A. (1995). The tonotopic map in the embryonic chicken cochlea. *Hear. Res.* **82**, 149–157.
- Kozak, M. (1991). An analysis of vertebrate mRNA sequences: intimations of translational control. *J. Cell Biol.* **115**, 887–903.
- Lagrutta, A., Shen, K.-Z., North, R.A., and Adelman, J.P. (1994). Functional differences among alternatively spliced variants of *Slowpoke*, a *Drosophila* calcium-activated potassium channel. *J. Biol. Chem.* **269**, 20347–20351.
- Latorre, R., Oberhauser, A., Labarca, P., and Alvarez, O. (1989). Varieties of calcium-activated potassium channels. *Annu. Rev. Physiol.* **51**, 385–399.
- Lewis, R.S., and Hudspeth, A.J. (1983a). Voltage- and ion-dependent conductances in solitary vertebrate hair cells. *Nature* **304**, 538–541.
- Lewis, R.S., and Hudspeth, A.J. (1983b). Frequency tuning and ionic conductances in hair cells of the bullfrog's sacculus. In *Hearing—Physiological Bases and Psychophysics*, R. Klinke and R. Hartmann, eds. (Berlin: Springer-Verlag), pp. 17–22.
- Li, M., Jan, Y.N., and Jan, L.Y. (1992). Specification of subunit assembly by the hydrophilic amino-terminal domain of the Shaker potassium channel. *Science* **257**, 1225–1230.
- Manley, G.A. (1990). The peripheral hearing organ of birds. In *Peripheral Hearing Mechanisms in Reptiles and Birds* (Berlin: Springer-Verlag), pp. 206–252.
- Manley, G.A. (1996). Ontogeny of frequency mapping in the peripheral auditory system of birds and mammals: a critical review. *Auditory Neurosci.* **3**, 199–214.
- Manley, G.A., Brix, J., and Kaiser, A. (1987). Developmental stability of the tonotopic organization of the chick's basilar papilla. *Science* **237**, 655–656.
- Manley, G.A., Gleich, O., Kaiser, A., and Brix, J. (1989). Functional differentiation of sensory cells in the avian auditory periphery. *J. Comp. Physiol. A* **164**, 289–296.
- Margolskee, R.F., McHendry-Rinde, B., and Horn, R. (1993). Panning transfected cells for electrophysiological studies. *Biotechniques* **15**, 906–911.
- McCobb, D.P., Fowler, N.L., Featherstone, T., Lingle, C.J., Saito, M., Krause, J.E., and Salkoff, L. (1995). A human calcium-activated potassium channel gene expressed in vascular smooth muscle. *Am. J. Physiol.* **269**, H767–H777.
- McManus, O.B., Helms, L.M.H., Pallanck, L., Ganetzky, B., Swanson, R., and Leonard, R.J. (1995). Functional role of the  $\beta$  subunit of high conductance calcium-activated potassium channels. *Neuron* **14**, 645–650.
- Murrow, B.W. (1994). Position-dependent expression of potassium currents by chick cochlear hair cells. *J. Physiol.* **480**, 247–259.
- Murrow, B.W., and Fuchs, P.A. (1990). Preferential expression of transient potassium current (*I<sub>t</sub>*) by 'short' hair cells of the chick's cochlea. *Proc. R. Soc. Lond. B* **242**, 189–195.
- Navaratnam, D., Escobar, L., Covarrubias, M., and Oberholtzer, J.C. (1995). Permeation properties and differential expression across the auditory receptor epithelium of an inward rectifier K<sup>+</sup> channel cloned from the chick inner ear. *J. Biol. Chem.* **270**, 19238–19245.
- Navaratnam, D.S., Bell, T.J., Tu, T.D., Cohen, E.L., and Oberholtzer, J.C. (1997). Differential distribution of Ca<sup>2+</sup>-activated K<sup>+</sup> channel splice variants among hair cells along the tonotopic axis of the chick cochlea. *Neuron*, this issue, **19**, 1077–1085.
- Nuovo, G.J. (1996). *PCR in situ Hybridization. Protocols and Applications*, 2nd Ed. (Philadelphia: Lippincott-Raven).
- Oberholtzer, J.C., Buettger, C., Summers, M.C., and Matschinsky, F.M. (1988). The 28-kDa calbindin-D is a major calcium-binding protein in the basilar papilla of the chick. *Proc. Natl. Acad. Sci. USA* **85**, 3387–3390.
- Pallanck, L., and Ganetzky, B. (1994). Cloning and characterization of human and mouse homologs of the *Drosophila* calcium-activated potassium channel gene, *slowpoke*. *Hum. Mol. Genet.* **3**, 1239–1243.
- Pinna, L.A., and Ruzzene, M. (1996). How do protein kinases recognize their substrates? *Biochim. Biophys. Acta* **1314**, 191–225.
- Roberts, W.M., Robles, L., and Hudspeth, A.J. (1986). Correlation between the kinetic properties of ionic channels and the frequency of membrane-potential resonance in hair cells of the bullfrog. In *Auditory Frequency Selectivity*, B.C.J. Moore and R.D. Patterson, eds. (New York: Plenum Press), pp. 89–95.
- Roberts, W.M., Howard, J., and Hudspeth, A.J. (1988). Mechano-electrical transduction, frequency tuning, and synaptic transmission by hair cells. *Annu. Rev. Cell Biol.* **4**, 63–92.
- Roberts, W.M., Jacobs, R.A., and Hudspeth, A.J. (1990). Colocalization of ion channels involved in frequency selectivity and synaptic transmission at presynaptic active zones of hair cells. *J. Neurosci.* **10**, 3664–3684.
- Rubel, E.W. (1984). Ontogeny of auditory system function. *Annu. Rev. Physiol.* **46**, 213–229.
- Rubel, E.W., Lippe, W.R., and Ryals, B.M. (1984). Development of the place principle. *Ann. Otol. Rhinol. Laryngol.* **6**, 609–615.
- Senapathy, P., Shapiro, M.B., and Harris, N.L. (1990). Splice junctions, branch point sites, and exons: sequence statistics, identification, and applications to genome project. *Methods Enzymol.* **183**, 252–278.
- Shen, N.V., Chen, X., Boyer, M.M., and Pfaffinger, P.J. (1993). Deletion analysis of K<sup>+</sup> channel assembly. *Neuron* **11**, 67–76.
- Shuster, M.J., Camardo, J.S., and Siegelbaum, S.A. (1991). Comparison of the serotonin-sensitive and Ca<sup>2+</sup>-activated K<sup>+</sup> channels in *Aplysia* sensory neurons. *J. Physiol.* **440**, 601–621.
- Strähle, U., Blader, P., Adam, J., and Ingham, P.W. (1994). A simple and efficient procedure for non-isotopic *in situ* hybridization to sectioned material. *Trends Genet.* **10**, 75–76.

- Subramony, P., Raucher, S., Dryer, L., and Dryer, S.E. (1996). Post-translational regulation of Ca<sup>2+</sup>-activated K<sup>+</sup> currents by a target-derived factor in developing parasympathetic neurons. *Neuron* **17**, 115–124.
- Takeuchi, S., Marcus, D.C., and Wangemann, P. (1992). Ca<sup>2+</sup>-activated nonselective cation, maxi K<sup>+</sup>, and Cl<sup>-</sup> channels in apical membrane of marginal cells of stria vascularis. *Hear. Res.* **61**, 86–96.
- Tanaka, K., and Smith, C.A. (1978). Structure of the chicken's inner ear: SEM and TEM study. *Am. J. Anat.* **153**, 251–272.
- Tilney, L.G., Tilney, M.S., Saunders, J.S., and DeRosier, D.J. (1986). Actin filaments, stereocilia, and hair cells of the bird cochlea. III. The development and differentiation of hair cells and stereocilia. *Dev. Biol.* **116**, 100–118.
- Tilney, L.G., DeRosier, D.J., and Tilney, M.S. (1992). Actin filaments, stereocilia, and hair cells: how cells count and measure. *Annu. Rev. Cell Biol.* **8**, 257–274.
- Tseng-Crank, J., Foster, C.D., Krause, J.D., Mertz, R., Godinot, N., DiChiara, T.J., and Reinhart, P.H. (1994). Cloning, expression, and distribution of functionally distinct Ca<sup>2+</sup>-activated K<sup>+</sup> channel isoforms from human brain. *Neuron* **13**, 1315–1330.
- von Bekésy, G. (1960). *Experiments in Hearing* (New York: McGraw-Hill).
- Wallner, M., Meera, P., and Toro, L. (1996). Determinant for β-subunit regulation in high-conductance voltage-activated and Ca<sup>2+</sup>-sensitive K<sup>+</sup> channels: an additional transmembrane region at the N terminus. *Proc. Natl. Acad. Sci. USA* **93**, 14922–14927.
- Wang, Z.-W., Nara, M., Wang, Y.-X., and Kotlikoff, M.I. (1997). Redox regulation of large conductance Ca<sup>2+</sup>-activated K<sup>+</sup> channels in smooth muscle cells. *J. Gen. Physiol.* **110**, 35–44.
- Wilson, P.W., Harding, M., and Lawson, D.E.M. (1985). Putative amino acid sequence of chick calcium-binding protein deduced from a complementary DNA sequence. *Nucleic Acids Res.* **13**, 8867–8881.
- Wu, Y.-C., and Fettiplace, R. (1996). A developmental model for generating frequency maps in the reptilian and avian cochleas. *Biophys. J.* **70**, 2557–2570.
- Wu, Y.-C., Art, J.J., Goodman, M.B., and Fettiplace, R. (1995). A kinetic description of the calcium-activated potassium channel and its application to electrical tuning of hair cells. *Prog. Biophys. Mol. Biol.* **63**, 131–158.
- Zidanic, M., and Fuchs, P.A. (1995). Kinetic analysis of barium currents in chick cochlear hair cells. *Biophys. J.* **68**, 1323–1336.

#### GenBank Accession Number

The accession number for the *cSlo* cDNA sequence is U73189.